CHARACTERIZATION OF SLUG FLOWS IN HORIZONTAL PIPING BY SIGNAL ANALYSIS FROM A CAPACITIVE PROBE

Emerson dos Reis
emersonr@fem.unicamp.br

Leonardo Goldstein Júnior
College of Mechanical Engineering of State University of Campinas, FEM / DETF / UNICAMP
Campus Zeferino Vaz, Barão Geraldo - Campinas, S. P., Brazil - Zip Code 13.083-970.
leonardo@fem.unicamp.br

Abstract. *The slug flow is a very common occurrence in gas-liquid two-phase pipe flow. Usually it is an undesirable flow pattern since the existence of long lumps of liquid slug that moves at high speed is unfavorable to gas-liquid transportation, and considerable efforts have been devoted to the prediction of the slug hydrodynamics characteristics. In this work, a capacitive probe was used to realize dynamic measurement in horizontal air-water slug flows under several flow rates. Instead of merely the holdup or void fraction in a finite volume of the flow, those signals represented the liquid layer thickness at near to every cross sectional area of the flow, since the probe had a thin sensing electrode that minimizes the axial length effect on the measurements. Tests were performed in a horizontal acrylic 34 mm ID pipe with 5m of length; in which not only slug flow regime but also stratified smooth and wavy flow were generated. Signal analysis techniques, as Power Spectrum Density (PSD) from Fourier Transform and Probability Density Function (PDF) from statistical analysis, were applied to the coming signals from the probe, and several two-phase flow characteristics were evaluated. Those techniques were compared when the flow regime identification is intended.*

Keywords. *Capacitance Probe, Liquid Thickness Measurement, Signal Analysis, FFT, PDF, Flow Regime Identification.*

1. Introduction

The complicated and complex nature of the two-phase has challenged researchers for the past few decades and also dictates the significance of experimental research in the areas of system design and development and phenomenological research. The experimental research, documentation, and control of real mixture flow require detection, monitoring and measurement *in situ* of many parameters associated with concentration and pressure with their signals in time and space. Based on monitoring static and dynamic components of pressure and concentration of the flow, many researches have devoted efforts to develop unambiguous techniques for flow regime identification, and toward characterization of those two-phase flows from dynamic signals (Mi *et al.,* 2001).

The slug flow particularly is one of the most common two-phase flow regimes over all inclination of the pipeline. It is characterized by an intrinsic unsteadiness due to alternating of liquid 'slugs' containing small bubbles and filling the whole pipe cross section, and of regions in which the flow consists of a liquid layer over/around (horizontal/vertical) a elongated gas bubble. Its intermittent behavior causes high fluctuations of pressure, concentration and also flow rate, so that an extremely careful design of the pipeline (valves, orifices, etc.) is required. Moreover, the low-frequency values of the slugs (few hertz) may be in resonance with the characteristic frequency of the pipeline itself, causing serious damages if not taken into account. Therefore, it is of essential importance not only to identify the slug flow regime but also determine its main characteristics, which should be useful for the engineer in design and process control.

Both pressure and concentration fluctuations that result from the passage of gas and liquid pockets, and their statistical characteristics, are particularly attractive for objective characterization of flow because the required sensors are robust, inexpensive and relatively well-developed, and therefore more likely to be applied in the industrial systems. From pressure fluctuations recorded by two transducers installed in a vertical pipeline, Franca *et al.* (1991) studied power spectral density (PSD) and the probability density function (PDF), and more recently by Shim and Jo (2000), for regime identification in gas–liquid two-phase flows. Based on the analysis of experimental data in a horizontal pipe, Franca *et al.* (1991) noted that, although PSD and PDF could not easily be used for regime identification, objective discrimination between separated and intermittent regimes might be possible by fractal techniques. Based on PSD and PDF analyses, Shim and Jo could characterize bubbly, churn, and slug flow patterns in low-flow experiments in a vertical pipe. At high flow rates, however, their technique could only distinguish the bubbly flow regime. Furthermore, especially using capacitive methods in concentration measurements, Geraest and Borst (1988), Das and Pattanayak (1993), Costigan *et al*. (1997) and Elkow and Rezkallah (1997) used similar techniques to identify the flow regimes. The authors reported successfully application of PDF when the flow rates of the liquid and gas phases are low, however, little attention have been paid in using PSD, mainly due to fact that the capacitance electrodes commonly are thin in axial flow direction (about 2 times the pipe diameter) which should enhance its sensitivity, and reduce the effect of electrical field distortion on the electrode's edges (Cimorelli and Evangelisti, 1967 and Elkow and Rezkallah, 1997).

However, if the probe is longer in the axial flow direction it can operate as a low pass filter that cutoff high frequencies related to the mixture flow as discussed by Reis and Goldstein (2005). It must be notice that this problem is not present when measuring pressure fluctuations. However, the most suitable type of transducer for this application is the piezoresistive (Wu *at al*., 2001, Elperin and Klochko, 2002), which measure only the dynamic component of pressure (Hjelmgren, 2002) and, consequently, part of the useful information may be lost if another one of different type was not used. Therefore, the system complexity should be increased.

In this work, the capacitive probe presented by Reis and Goldstein (2003) was used to acquire data related to the liquid layer thickness from horizontal air-water two-phase flows under slug flow, stratified smooth and wavy flow regimes. Further PDF and PSD analysis of data, which are very known techniques for signal analysis, allowed the evaluation of several flow characteristics.

2. Experimental Installation

Figure 1 shows a schematic of the experimental flow loop. The air supply system is composed of a reciprocating compressor, producing 19.1 m^3/h at 830 kPa, an air reservoir, *AR*, of 400 liters, to reduce pressure oscillations downstream, an air filter and pressure regulator, two needle valves, *VC1* and *VC2*, one for fine flow adjustment, and two turbine flow meters, *TM1* and *TM2*, of 3/4 and 1 1/2 inches, for measurement of the volumetric airflow rate, Q_G, with ranges from 1.1 to 11.0 and 8.8 to 88.0 m^3/h, and calibrated measurement uncertainties of ± 0.14 m^3/h and ± 0.41 m^3/h, respectively. A type T thermocouple, *T1*, and an electronic pressure gauge, *P1*, were used to measure the air temperature and manometric pressure.

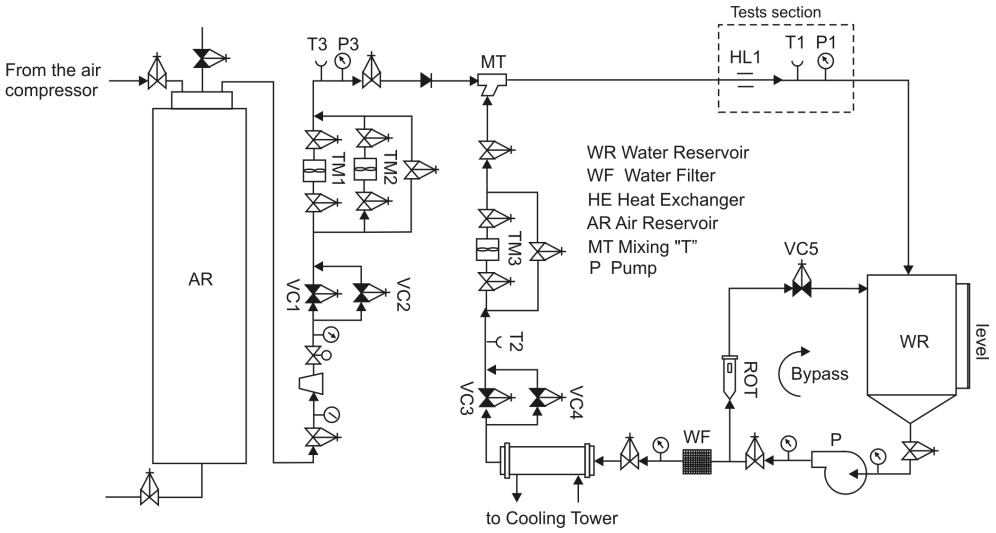

Figure 1. Experimental installation schematic

The water supply system was composed of a reservoir, *WR*, which also performed air-water separation; a centrifugal pump, *P*, with a capacity of 45 m^3/h at 274 kPa (75% efficiency); two water filters, *WF*, operating in parallel; a double tube heat exchanger, *HE*; two control valves, *VC3* and *VC4*, one for fine adjustment, and a turbine meter, *TM3* for measure the volumetric water flow rate, Q_L, which ranged from 3.0 to 45 l/min, with a measurement uncertainty of ± 0.23 l/min. A water-cooling system became necessary due to heating of the circulating liquid. A cooling tower supplied water close to the wet bulb temperature to the annular side of the heat exchanger. Tests were made with deionized water to avoid fouling the internal pipe walls, meters and valves. A type T thermocouple was used to measure the water temperature, *T2*.

The air-water flow system was composed by an 13 m long Plexiglas pipeline with an internal diameter, *D*, of 34 mm and a 3 mm of wall thickness, a junction with 45° branch arms, *TM*, which mixed air and water at the mixture point. The Plexiglas pipeline has about 5 m of length from *MT* to the tests section (150 *D*). Type T thermocouples were used to measure the temperature of air-water mixture, *T1*. A data acquisition system composed of a microcomputer, AT-MIO-16E10 board, connections block, and Labview 5.0, by National Instruments ™, was used to log all data from instruments.

3. Capacitive Probe Description

As discussed by Reis and Goldstein (2003), the measurement device of liquid film thickness, h_L, is composed of an electrode capacitive sensor, sinusoidal signal source and capacitance transducer circuit, as showed in Fig. 2. Sensing electrode is that connected to the capacitance transducer and source electrode is that connected to sinusoidal signal source. The sensing electrode has a minimum width of 3 mm (black); it allows the probe to detect high frequencies

related to the gas-liquid flow and almost only the liquid into the sectional volume limited by the sensing electrode to affect the capacitance transducer response. Two guard electrodes mounted very close to sensing electrode (0.5 mm) avoids the electric field distortion near to the sensing electrode edges, called border effect (Reinecke and Mewes, 1996). The electric fields formed among the sensor electrode and guard electrodes are null due to the virtual ground condition imposed during the design of the capacitance transducer circuit (Yang, 1994). As smaller sensing electrode width as closer the system response to the liquid thickness measurement taken exactly in the sectional tube area (fact that is interesting in the measure of waves amplitude). In that sense, the technique limitation is due to the sensibility and speed response of the capacitance transducer circuit. Reis (2003) presented an analog transducer circuit suitable for this application. The sensibility was evaluated equal to 7.0 mV/fF and the circuit settling time about 6 ms.

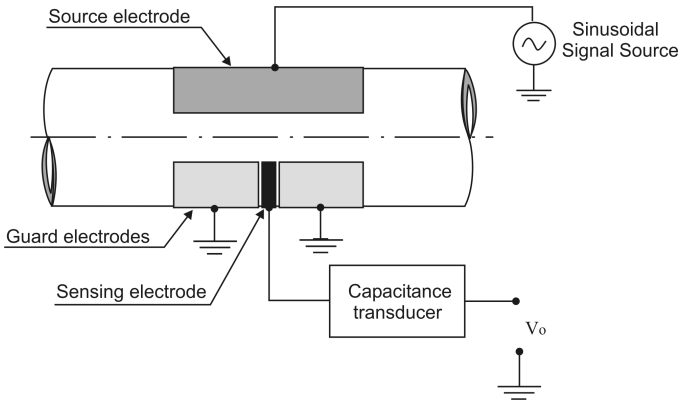

Figure 2. Thin electrode capacitance probe

Reis and Goldstein (2005b) presented a similar probe of Fig. 2, however, it had two sensing electrodes connected to a capacitive transducer circuit with independent channels, which allow simultaneous measurements of both the liquid layer thickness and the flow velocity by applying cross correlation technique to the coming signals.

4. Experimental Procedure and Data Reduction

Figure 3 presents the theoretical air-water flow map for the horizontal pipe of 34 mm of diameter, *D* (Taitel and Dukler, 1976). The light gray square delimits the flow tests region, while the dark gray polygon delimits the slug flow test region. Thirteen flow conditions were tested into the slug, stratified smooth and stratified wavy flow regimes, as shown in the flow map of Fig. 3, which some of these flow conditions were taken near to the slug-stratified and slug–annular transition lines. Therefore, the air injection system of the test apparatus was fitted with a control valve and two turbine meters, which enabled covering the air superficial velocities, $u_{GS} = Q_G/A$, in the range from 1.3 to 6.0 m/s. The water flow had a single turbine meter system that allowed water superficial velocities, u_{LS}, in the range from 0.08 to 0.80 m/s.

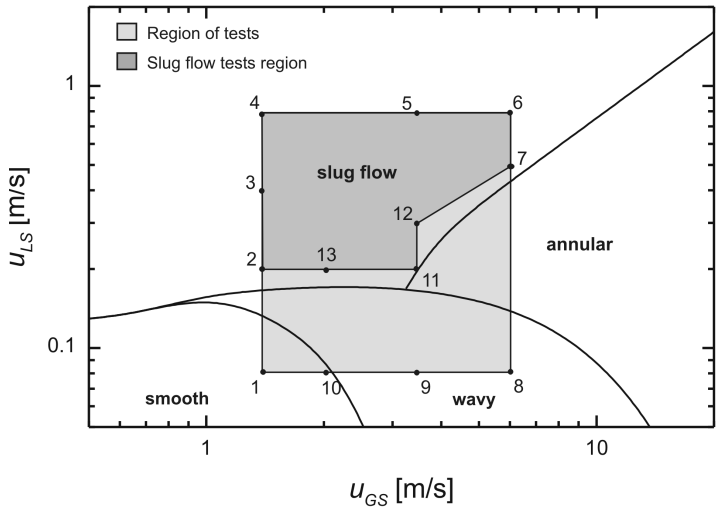

Figure 3. Flow regime map (*D* = 34.0 mm)

Flow rates of air and water through *TM1* or *TM2* and *TM3*, shown in Fig. 1, manometric pressure and temperature of the air-water flow mixture, *P1* and *T1*, temperature of water *T2*, temperature of air, *T3*, and signals from

the capacitive probe, *HL1*, all them were logged by the data acquisition system and stored in a digital file. Moreover, before define the acquisition time, t_a, equal to 300s for each test (5 minutes), the number of samples, n, and the data acquisition rate, f, were adjusted to maintain the acquisition time equal in all tests. The f value was chosen equal to 800 Hz for tests 1, 2, 3, 4, 9, 10 and 13 having the smaller flow velocities (~1.5 m/s), 1500 Hz for points 5, 8, 11, and 12, and 2500 Hz for points 6 and 7 having the highest flow velocities (~6.5 m/s). This corresponded, for example, to n = 240000 samples acquired at 800 Hz. The use of high data acquisition rates was due to the temporal resolution of the signals demanded by the cross correlation technique, which was used by Reis and Goldstein (2005b) to measure the mean translational velocity of the slug flows. This fact cannot cause any problem for PSD or PDF analysis, since more information must only become increased the computational work.

In the data reduction stage, all acquired signals related to electrical voltages from temperature, volumetric flow rate and pressure meters were first averaged, and converted to measured values by the calibration curve of each instrument; following the fluids properties and mass flow rate in the feeding lines were determinate. Differently, all acquired signals from the capacitive probe were converted to the respective non-dimensional liquid film thickness measurements, h_L/D, also by using the calibration curve, and they received a corrective technique due to the deviations of the dielectric permittivity of water due to the flow temperature variations (Reis and Goldstein, 2005a). Again the h_L/D values in number of n were stored in a digital file.

In the signal analysis stage, all h_L/D data processing was started with the raw data that was ten-point filtered to remove noise (moving average filter). After that, the Probability Density Function - PDF (Walpole and Myers, 1972) was easily found by the construction of histograms, which each one had 30 intervals of over the range from minimum to maximum value registered of h_L/D. From the histograms, the probability of each interval, i, was $P(h_L/D)_i$ = (number of values of h_L/D into the interval i) / number of samples, n. Following the Power Spectrum Density – PSD was calculated from the fast-Fourier transform-FFT as the magnitude of the complex numbers from 1 to n/2+1 (Oppenheim *et al*., 1997, Smith, 1999). Data of h_L/D were used in FFT without filtering, and following the PSD data was 20-point filtered to remove noise from the longer FFT and provide a good frequency resolution. The PSD graphs were produced without the single component at 0 Hz, and from 0 to 6 Hz that concentrates almost whole the power spectrum in all tests. A computational program in Fortran 90 was built for these whole processes of data reduction and treatment.

5. Results and Discussion

Figures 5 to 7 show three types of graphs for each test showed in the map of Fig. 3 from 1 to 13: a sample graph of h_L/D over a 30s at left, a PDF at center, and PSD at right. From visual observations, signals produced by the probe in tests 2, 3, 4, 5, 6, 7, 11, 12 and 13, in Fig 4 and 5 were under flow regime identified as slug, while in tests 1, 8, 9 and 10 the flow regime was identified as stratified smooth in 1 and wavy in 8, 9, and 10, which is in agreement with the map of Fig. 3. Furthermore, the following data analyses will trail the diagram show in Fig. 4, which are concerned about the variation of air and water flow rates or superficial velocities among the tests and represents the polygon shown in Fig. 3. The graph was divided in two parts according to the flow patterns: stratified or slug, and it started from test 2, which represent the lowest superficial velocities of both phases among the tests under slug flow, to tests 3 and 4 with higher liquid and lower gas flow rate, and to tests 5 and 6 with higher liquid and gas flow rates, and to the test near to the slug-annular and slug-stratified flow regime transition lines, in the clockwise path indicated by the arrows. Further analysis of stratified flow data will start from test 1 to the test 8 with highest airflow rate, while the water flow rate was kept constant. Still Fig. 4 shows a scheme of the horizontal Plexiglas pipeline and the capacitive probe on the test section.

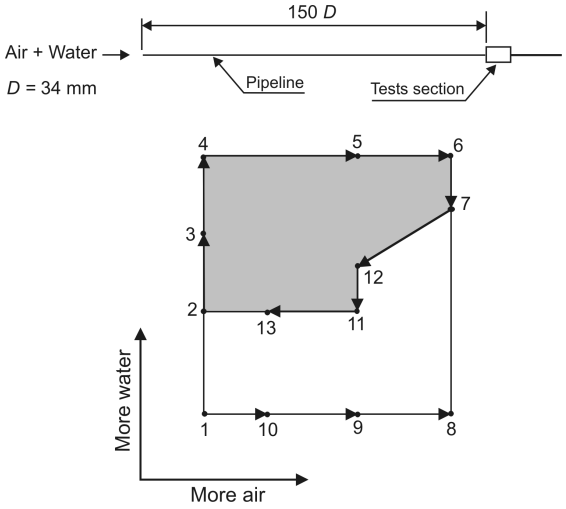

Fig. 4. Scheme of data analysis

An analysis of data from slug flows should be given considering the amount of liquid flowing in the pipe increasing from the test 2 to 4 about 300%, while the airflow rate was kept constant. Firstly, signal samples of tests 2, 3 and 4 in Fig. 4 indicate the presence of liquid slugs when h_L/D is near to 1.0, and regions of the elongated gaseous bubbles with lower values of h_L/D separating them. The PDF graphs show the h_L/D signals in a large range from about 0.25 to 1.0, however, the liquid layer above the elongated bubbles become ticker from h_L/D = 0.12 in 2 to h_L/D = 0.25 in 4. Therefore, the main characteristic of the PDF graphs is the presence of two peaks with a central region of lower signal probability. One these peaks is placed at about h_L/D = 0.4, and the another one at near to h_L/D = 1.0. They indicate the presence of two important values of h_L/D: the left one is related to the presence of the elongated bubbles air-water interface and the right one to the liquid slugs. The peaks at left, in general, are greater them the right ones, however, one should observe an increase of peaks at right from test 2 to 4, and also the probability of the signals into the region between the two peaks was also increased, causing a more regular distribution of probability. Furthermore, the presence of the hydraulic jump can be observed in test 2 and 3, and a reduction of high waves into the elongated bubbles from 2 to 4. A “mountain” shape characterizes the PSD graph for slug flow with a highest peak corresponding to the dominant frequency. Therefore, it is observed the dominant frequency increasing from about 0.1 Hz in 2, passing by 0.5 Hz in 3, and reaching 1.2 Hz in 4, as could be expected from signal sample graphs.

The liquid flow rate was kept high and constant from test 4 to 6, while the airflow was increased about 360%. Thus, it can be observed in the signal sample graphs of tests 5, 6 and 7, signals of h_L/D reaching 1.0 rarely when occurred the passage of liquid slugs, as in tests 2, 3 and 4. This fact is associated to the increase of the presence of small gaseous bubbles dispersed into the liquid slug body, since the capacitive measurement system is affected by their presence, which is proportional to the effective dielectric permittivity of the mixture, and their population is greater as the flow velocity is increased together with the airflow rate and, consequently increasing the void fraction into the slugs. By the way, the range of h_L/D was not different from the first ones, however, the PDF graphs show the disappearance of the right peaks of the liquid slugs from 4 to 6 due to the peaks on h_L/D signals became sharper, while the probability of the left region was increased, but with the same width. This gave to the PDF the form of a chi-square probability distribution. Therefore, high waves were also into the elongated bubbles region, as can be see in signals of test 5 and 6, being they increased from test 4 to 6 that was the opposite way of from test 2 to 4. However, due to the presence of highly aerated slugs in test 6, some confusion about what is slug and wave should be present. Therefore, the PDF graphs also show a reduction of the thickness liquid layer below the elongated bubbles from h_L/D = 0.25 in 4 to 0.13 in 6. The graphs of PSD present the same “mountain” shape; however, with a larger decrease of the spectrum range to about half of tests 2, 3 and 4, together with the appearance of some components of higher frequency from test 2 to 5 and 6. Furthermore, the PDSs show the dominant frequency being decreased from test 4 at about 1.2 Hz to 1.0 Hz in 5 and increasing again to 1.8Hz in Test 6, consequently this fact should state the frequencies related to the hydrodynamics of the air-water slug flow as do not representing an univocal function of the liquid and gas flow rates or superficial velocities.

The liquid flow rate was decreased about 60% from test 6 to 7, while the airflow rate was kept high, as shown in Figs. 5 and 6. Consequently, the flow condition on test 6 was near to the slug-annular transition line, as shown in Fig. 3, and the signal sample graphs show, both a reduction of the peaks on the h_L/D signals, which show the slugs as more aerated than 6, and an increase of the time interval among those peaks. Therefore, it should be deduced an increase of high waves presence on the flow. The PDF graphs are very similar while the PSD graphs show a small reduction of the spectrum range, with the dominant frequency falling from 1.8 Hz in test 6 to about 1.3 Hz in test 7.

Both air and water flow rates were reduced from 7 to 12 about 82% and 66%, respectively, and de signal sample graphs show no huge change on the flow hydrodynamics, since the peaks on h_L/D became more spaced on time but they still aren’t high at about h_L/D = 1.0 and the presence of waves is predominant, as can be seen in PDF graphs, which both having the same shape. However, huge changes occurred on the frequencies of signals as shown in the PSD graphs, with a decrease of the shape and the dominant frequency becoming smaller from 1.3 Hz in 7 to about 0.5 Hz in 12.

The liquid from rate was decreased again from test 12 to 11 about 100%, while the airflow rate was the same. In a general way all, graphs of tests 12 and 11 are similar: signal sample, PDF and PSD, and also the graphs of test point 13 when the airflow rate was decreased from test 11 about 65%, however, the PDF graph of test 13 shown the appearance of the right peak related to the liquid slug region, showing the presence of less aerated slugs as occurred in tests 2, 3, 4 and 5.

Tests 1, 10, 9 and 8 are into the stratified smooth and stratified wavy flow regime as shown in the map of Fig. 3, and this fact can be observed on graphs of sample signal shown in Fig. 7, since the gaseous phase flow over the liquid one separately. Therefore, the airflow rate was increased from test 1 to 8 about 360 % while the water flow rate was kept about 150% below that one of tests 2, 13 and 11 under slug flow. The signal sample graph of test 1 show almost a straight line of h_L/D at about 0.42 along the time, and the PDF graph represents a single stripe at 0.42, while the PSD graph show this flow condition as having some component of frequency different from 0 Hz, however, they are smaller due to the range of the spectrum, and this graph have two distinct region: one at low frequency range with dominant frequency at about 0.1 Hz at left; and another with a scattered spectrum about a the dominant frequency at 4 Hz at right. Moreover, the increase of the airflow rate also increased the oscillations on the air-water interface from 1 to 9, as can be seen in the signal samples PDF graphs, which present a greater range of h_L/D from 1 to 9, and a reduction of the mean thickness layer of liquid from h_L/D = 0.42 to 0.30. The PSD graphs of tests 10 and 9 show a considerable increasing of amplitude of the waves, since the power spectrum range had increased barely, while their shape was similar to the test 1

with two distinct regions although the PSD graph of test 10 shows a small component of low frequency on the left region, and that one of test 9 shows a scattered range of frequencies on the right region. It also shows the large range of frequencies of the interface in test 9 with dominant frequency about 5.8 Hz, which was narrower in test 10 with a dominant frequency about 4.5 Hz.

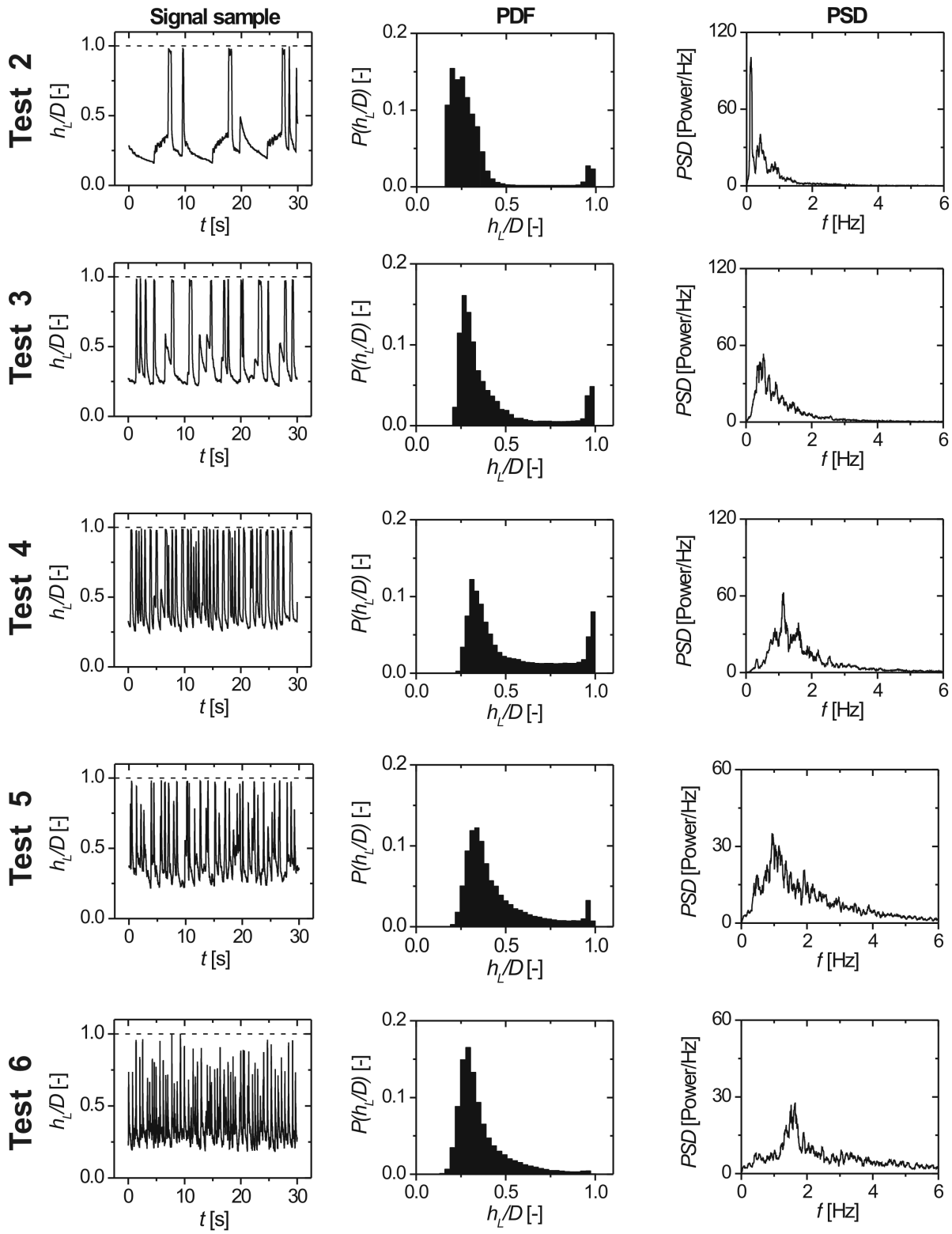

Figure 5. Graphs of tests under slug flow – Tests 2 to 6

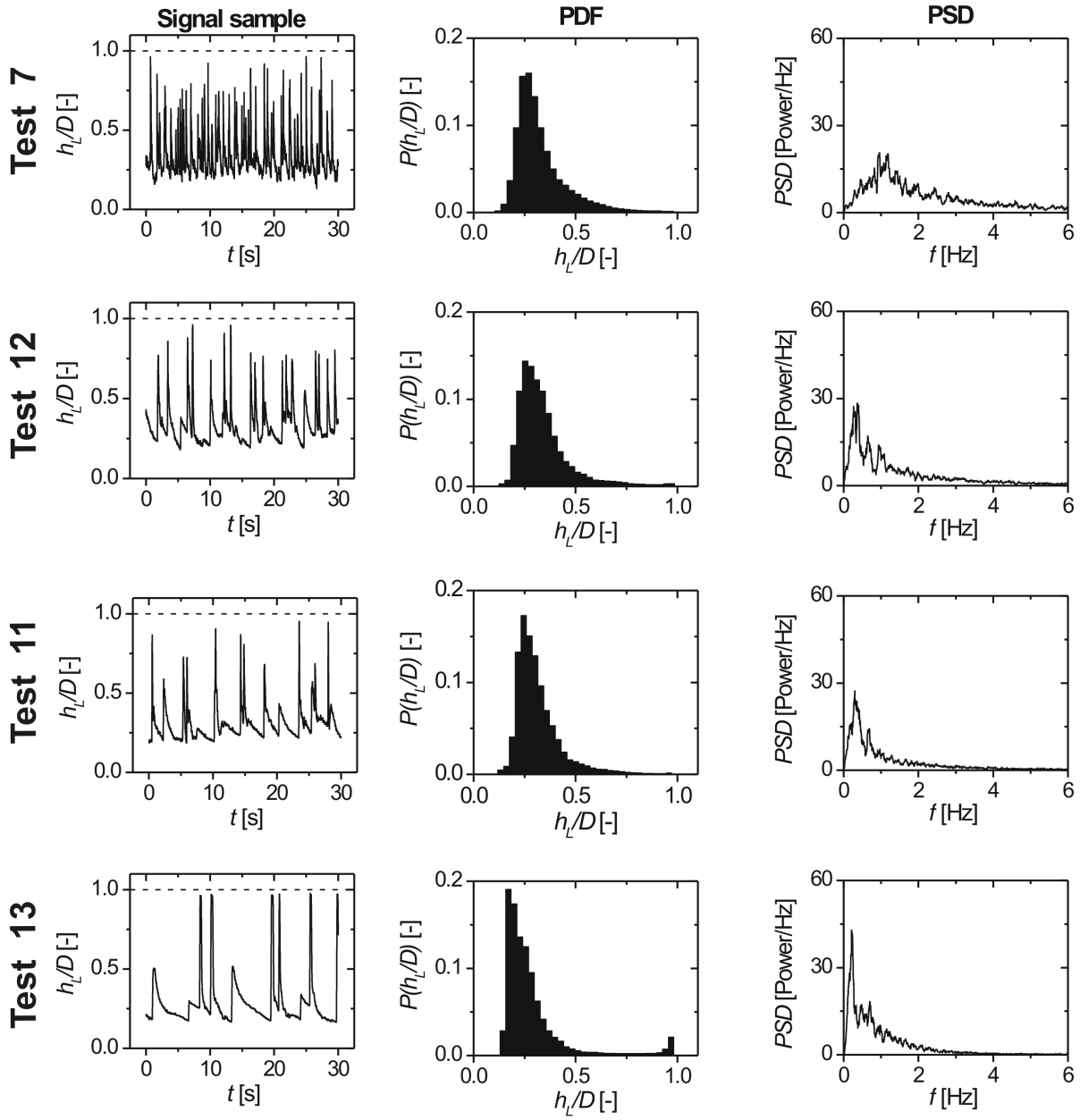

Figure 6. Graphs of tests under slug flow – Tests 7 to 13

The airflow rate was also increased about 82% from test 9 to 8. The waves became higher and the liquid layer become thinner, as seen in the signal sample PDF graphs. However, the PDF graph is very similar to those of tests 6 to 11, with a probability distribution seemed like a chi-square, which may cause some confusion at least that both condition have different ranges of h_L/D. Still the PDS graph seems like those ones of tests 2, 12, 11 and 13 under slug flow regime that were near to the slug-stratified transition line, and with a dominant frequency at about 0.8 Hz that also is near to those ones.

Consequently, the analysis of data presented above should be useful in determining the effectiveness of PDF and PSD techniques of signal analysis from a capacitive probe, which measure the liquid layer thickness h_L/D, when the flow pattern identification among stratified smooth, wavy and slug is required.

Although the PDF can presented a different form among stratified and slug flow, since it presented a single peak for stratified and two peaks for slug flow, as shown on the graph of tests 1, 10, 9, and 8, and 2 to 5, it is not true when the slug flow occurred under high airflow rate and the slugs become highly aerated. In this condition, the right peak on PDF graph can disappear and it seems like the graph of stratified wavy flow with higher airflow rate, test 8. Therefore, the PDF graphs were useful tools when analyzing the characteristics of the air-water flow studied, but they were not sufficient to state every flow regimes with safety.

The PDS graphs were also useful tools in analyzing the frequencies related to the flow, but they also presented some problems when identifying flow regimes under stratified wavy under high airflow rates, test 8, and slug flow near to the transition lines, tests 2, 12, 13,11, 13. However, the power spectrum range of slug flow were greater about 1500% of that from the wavy flows, which could be decisive when identifying the flow regime.

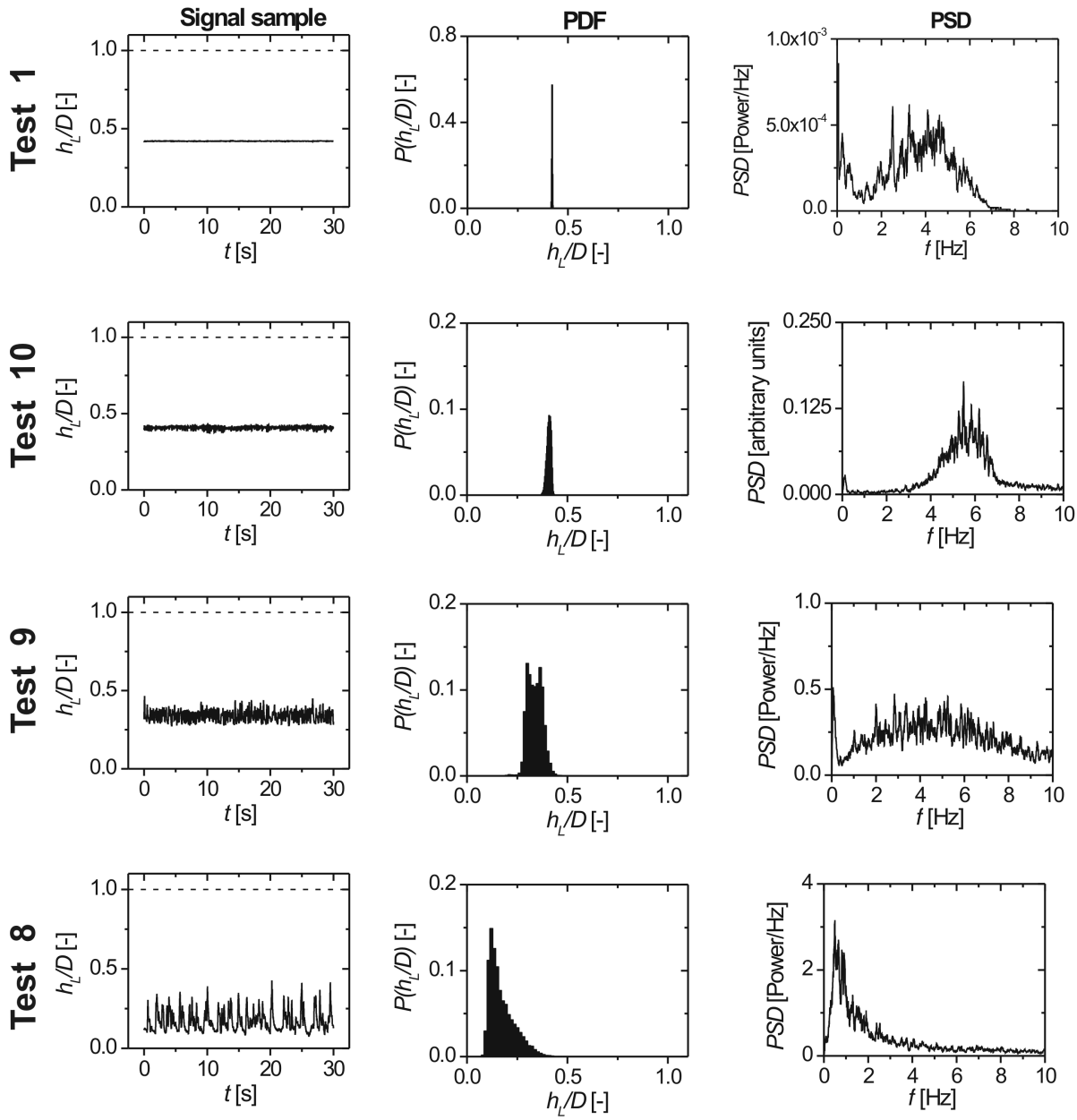

Figure 7. Graphs of tests under stratified smooth and way flow

6. Conclusion and Remarks

This paper presents a study about the signal analysis of a capacitive probe used to register data of the liquid layer thickness from air-water two-phase flows under stratified smooth, stratified wavy and slug flow regimes, which some of them were near to the transition lines on regime flow map. These flows were generated in a horizontal acrylic 34 mm of diameter pipeline, and the probe was installed at 150 *D* downstream from the phases mixing point. Both probability density function and fast-Fourier-transform were applied to the acquired signals, and graph of probability distribution – PDF – and power spectrum density – PDS – were presented.

Those graphs shown themselves as useful tools when evaluation the characteristics of the flows as: range of the liquid layer thickness, presence of waves, dominant frequencies, presence of hydraulic jump, regions of signals concentration, range of signal frequencies, amplitude. However, both techniques had presented graphs with similar

forms among stratified and slug flows, mainly when they occurred with high gas flow rates. However, the PDS graphs presented a more different range of the power spectrum than PDF of the liquid layer thickness, which could make possible the correct identification of those flows.

Finally, it must be considered the fact of the main disadvantage of the capacitive technique used, which could make confusion between high waves and highly aerated slugs of liquid. This could give the signals similar impressions that appeared on the PDF and PSD graphs.

7. Acknowledgement

The support of FAPESP – Fundação de Amparo à Pesquisa do Estado de São Paulo, Brazil, is deeply appreciated.

8. References

Cimorelli, L., Evangelisti, R., 1967, "The application of the capacitance meted for void fraction measurement in bulk boiling conditions", Heat and Mass Transfer, Vol. 10, pp. 277-288.

Costigan, G., Whalley, P. B., 1997, "Slug flow regime identification from dynamic void fraction measurements in vertical air-water flows", International Journal of Multiphase Flow, Vol. 23, n. 2, pp.263-282.

Das, R. K., Pattanayak, S., 1993, "Electrical impedance method for flow regime identification in vertical upward gas-liquid two-phase flow", Measurement Science and Technology, Vol. 4, n. 12, pp. 1457-1463.

Elkow, K. J., Rezkallah., K. S., 1996, "Void fraction measurements in gas-liquid flows using capacitance sensors", Measurement Science and Technology, Vol. 7, n. 8, pp. 1153-1163.

Franca, F., Acikgoz, M., Lahey Jr, R. T., Clausse, A., 1991, "The use of fractal techniques for flow regime identification", International Journal of Multiphase Flow, Vol. 17, n. 4, pp. 545-552.

Geraest, J. J. M., Borst, J. C., 1988, "A capacitance sensor for two-phase void fraction measurement and flow pattern identification", International Journal of Multiphase Flow, Vol. 14, n. 3, pp. 305-320.

Hjelmgren, J., 2002, "Dynamic Measurement of Pressure – .A Literature Survey", SP Swedish National Testing and Research Institute, Report 2002:34.

Oppenheim, A. V., Willisky, A. S, Nawab, S. H., 1983, "Signals and Systems", Prentice Hall, 2.ed, Upper Saddle River, New Jersey.

Reinecke, N., Mewes, D., 1996, "Recent developments and industrial/research applications of capacitance tomography", Measurement Science and Technology, Vol. 7 ,n. 3, pp. 233-246.

Reis, E. dos. 2003, Estudo do escoamento pistonado horizontal ar-água em tubulações com ramificação "T": School of Mechanical Engineering, State University of Campinas, 2003. PhD Thesis in portuguese.

Reis, E. dos, Goldstein Jr, L, 2003, "A new probe for measuring the gas-liquid interface profile in horizontal two-phase flows", Proceedings of the 17th International Congress of Mechanical Engineering, São Paulo, Brazil.

Reis, E. dos, Goldstein Jr. L., 2005a, "A procedure to correct the effect of fluid flow temperature variation on the response of capacitive void fraction meters", Flow Measurement and Instrumentation, Vol. 16, n. 4, pp. 267-274.

Reis, E. dos, Goldstein Jr. L., 2005b, "A non-intrusive probe for bubble profile and velocity measurement in horizontal slug flows", Flow Measurement and Instrumentation, Vol. 16, n. 4, pp. 229-239.

Shim, W., Jo, C. H., 2000, "Analysis of pressure fluctuations in two-phase vertical flow in annulus", Journal of Industrial and Engineering Chemistry (Seoul), Vol. 6, pp. 167-173.

Smith, S. W. *Digital Signal Processing*. California Technical Publishing, 2.ed, San Diego, California, 1999.

Taitel, Y., Dukler, A. E. 1976, "A model for predicting flow regime transitions in horizontal and near horizontal gas-liquid flow", AIChE Journal, Vol. 22, n. 1, pp. 47-55.

Walpole, R. E., Myers, R. H., 1972, "Probability and Statistics for Engineers and Scientists", The Macmillan Company, New York.

Wu, H., Zhou, F., Wu, Y., 2001, "Intelligent identification system of flow regime of oil-gas-water multiphase flow", Experiments in Fluids, Vol. 32, n. 6, 2002.

Yang, W. Q., Stott, A. L., Beck., M. S., 1994, "High frequency and high resolution capacitance measuring circuit for process tomography", IEE Proc.-Circuits Devices Sustems, Vol. 141, n. 3, pp. 215-219.